Algebraic Methods in Mechanism Analysis and Synthesis

Manfred L. Husty

University Innsbruck, Institute of Basic Sciences in Engineering,
Technikerstraße 13, A6020 Innsbruck, Austria
email:manfred.husty@uibk.ac.at

Abstract: Algebraic methods in connection with classical multidimensional geometry have proven to be very efficient in the computation of direct and inverse kinematics of mechanisms as well as the explanation of strange, pathological behavior. In this paper we give an overview of the results achieved within the last years using the algebraic geometric method, geometric preprocessing and numerical analysis. We provide the mathematical and geometrical background, like Study's parametrization of the Euclidean motion group, the ideals belonging to mechanism constraints and methods to solve polynomial equations. The methods are explained with different examples from mechanism analysis and synthesis.

1 Introduction

There are many different mathematical methods in dealing with mechanism analysis and synthesis. Matrix and vector methods are most common to derive equations that describe the mechanisms (see e.g. Angeles [1]). Generally these methods have the disadvantage, that one has to deal with sines and cosines, which are eliminated using half tangent substitutions. Within the last ten years algebraic methods have become successful in solving problems in mechanism analysis and synthesis. One of the main reasons are the advances in solving systems of polynomial equations. Many algorithms have been developed, all of them heavily relying on the use of computer algebra systems (see e.g. Dickenstein et.al. [8]).

In mechanism science is important to find the simplest mathematical modelling of a mechanism, because the systems of polynomial equations generally are very complicated. Therefore it seems to be advantageous to have additionally a geometrical setting for the interpretation of the equations. Kinematic image spaces provide such a setting. They have been introduced by W. Blaschke [5] and E. Study [24] and have been forgotten for long time. The main contribution of this overview paper is to show that geometric preprocessing and an understanding of the multidimensional geometry of kinematic image spaces is crucial to find simple sets of equations, which then can be solved efficiently using all the advances in computer algebra and the newly introduced methods in polynomial equation solving.

The paper is organized as follows: In the remaining part of the introduction the mathematical background and the algebraic-geometric method to derive constraint equations for mechanism analysis and synthesis is provided. Section 2 gives then the application of the devised algorithms to mechanism analysis, especially to the direct kinematics of Stewart-Gough platforms, self-motions of platform mechanisms and the inverse kinematics of serial $6R$-chains. Section 3 deals with the synthesis of Bennett mechanisms.

1.1 Study-Model of SE(6)

Euclidean displacements $\mathcal{D} \in SE(6)$ can be described by (see [13, 18])

$$\mathcal{D}\colon \mathbf{x}' = \mathbf{A}\mathbf{x} + \mathbf{t}, \tag{1}$$

where $\mathbf{x}'$ resp. $\mathbf{x}$ represent a point in the fixed resp. moving frame, $\mathbf{A}$ is a 3×3 proper orthogonal matrix and $\mathbf{t} = [t_1, t_2, t_3]^T$ is the translation vector, connecting the origins of moving and fixed frame. Expanding the dual quaternion representation (see [13, Section 3.3.2]) and using an operator approach, the matrix operator corresponding to the normalized dual quaternion $\mathbf{q} = [x_0, x_1, x_2, x_3] + \varepsilon[y_0, y_1, y_2, y_3]$ is given by

$$\mathbf{M} := \begin{bmatrix} 1 & 0 & 0 & 0 \\ t_1 & x_0^2 + x_1^2 - x_3^2 - x_2^2 & -2x_0x_3 + 2x_2x_1 & 2x_3x_1 + 2x_0x_2 \\ t_2 & 2x_2x_1 + 2x_0x_3 & x_0^2 + x_2^2 - x_1^2 - x_3^2 & -2x_0x_1 + 2x_3x_2 \\ t_3 & -2x_0x_2 + 2x_3x_1 & 2x_3x_2 + 2x_0x_1 & x_0^2 + x_3^2 - x_2^2 - x_1^2 \end{bmatrix}. \tag{2}$$

where

$$\begin{aligned} t_1 &= 2x_0y_1 - 2y_0x_1 - 2y_2x_3 + 2y_3x_2, \\ t_2 &= 2x_0y_2 - 2y_0x_2 - 2y_3x_1 + 2y_1x_3, \\ t_3 &= 2x_0y_3 - 2y_0x_3 - 2y_1x_2 + 2y_2x_1. \end{aligned} \tag{3}$$

The point $[x, y, z]^T$ is transformed to $[x', y', z']^T$ according to

$$[1, x, y, z]^T = \mathbf{M} \cdot [1, x', y', z']^T.$$

The entries $[x_i, y_i]$ in the transformation matrix $\mathbf{M}$ have to fulfill the quadratic identity

$$x_0y_0 + x_1y_1 + x_2y_2 + x_3y_3 = 0 \tag{4}$$

and at least one x_i is different from 0. The lower right 3×3 sub-matrix of $\mathbf{M}$ is an element of the special orthogonal group $SO(3)^+$ and the x_i are the Euler parameters. This representation of Euclidean displacements is sometimes called Study representation and the parameters x_i, y_i are called Study parameters. This allows the following multidimensional geometric interpretation: Eq. (4) defines a six dimensional quadric hyper-surface in a seven dimensional projective space P^7. This quadric S_6^2 is called *Study quadric* and serves as a point model for Euclidean displacements. The quadric S_6^2 is of hyperbolic type and has the following properties:

1. The maximal linear spaces on S_6^2 are three dimensional (generator spaces).

2. Each tangent space cuts S_6^2 in a five dimensional cone.

3. The generator space $x_0 = x_1 = x_2 = x_3 = 0$ is one of the 3-spaces mentioned above but it does not represent regular displacements, because in this space all Euler parameters are zero. Therefore this space has to be cut out of S_6^2. A quadric with one generator space removed is called sliced.

A detailed treatment of more properties of S_6^2 can be found in [23, Chapter 10]. The mapping

$$\begin{gathered} \kappa\colon \mathcal{D} \to P \in P^7 \\ \mathbf{M}(x_i, y_i) \to [x_0 : x_1 : x_2 : x_3 : y_0 : y_1 : y_2 : y_3]^T \neq [0:0:0:0:0:0:0:0]^T \end{gathered} \tag{5}$$

is called *kinematic mapping* and maps each Euclidean displacement $\mathcal{D}$ to a point P on $S_6^2 \subset P^7$.

Given a displacement $\mathcal{D}$ as in Eq. (1) it is straightforward to compute the Study parameters x_i, y_i. One can use one of the formulas (6) to compute the Euler parameters x_i directly from the 3×3 proper orthogonal matrix $\mathbf{A} = (a_{ij})_{i,j=1,\ldots,3}$:

$$\begin{aligned} x_0 : x_1 : x_2 : x_3 &= 1 + a_{11} + a_{22} + a_{33} : a_{32} - a_{23} : a_{13} - a_{31} : a_{21} - a_{12} \\ &= a_{32} - a_{23} : 1 + a_{11} - a_{22} - a_{33} : a_{12} + a_{21} : a_{31} + a_{13} \\ &= a_{13} - a_{31} : a_{12} + a_{21} : 1 - a_{11} + a_{22} - a_{33} : a_{23} + a_{32} \\ &= a_{21} - a_{12} : a_{31} + a_{13} : a_{23} + a_{32} : 1 - a_{11} - a_{22} + a_{33}. \end{aligned} \tag{6}$$

These formulas are already due to Study [24]. If $\mathbf{A}$ is non-symmetric, we can always take the first proportion of (6). If $\mathbf{A}$ is symmetric, then it describes a rotation about an angle of π and the first formula fails. In this case we can always resort to one of the three remaining proportions. It should be noted, that at least one of the four proportions in (6) is nonzero! The y_i are given by

$$\begin{aligned} y_0 &= -\frac{1}{2}(t_3x_3 + t_2x_2 + t_1x_1), & y_1 &= -\frac{1}{2}(t_3x_2 - t_2x_3 - t_1x_0), \\ y_2 &= -\frac{1}{2}(-t_3x_1 + t_1x_3 - t_2x_0), & y_3 &= -\frac{1}{2}(-t_3x_0 + t_2x_1 - t_1x_2). \end{aligned} \tag{7}$$

Remark 1 *Planar displacements and spherical displacements are included in the model presented above. The kinematic image of spherical displacements is obtained from* (2) *by setting* $y_i = 0$*:*

$$\mathbf{M} := \begin{bmatrix} 1 & 0 & 0 & 0 \\ 0 & x_0^2 + x_1^2 - x_3^2 - x_2^2 & -2x_0x_3 + 2x_2x_1 & 2x_3x_1 + 2x_0x_2 \\ 0 & 2x_2x_1 + 2x_0x_3 & x_0^2 + x_2^2 - x_1^2 - x_3^2 & -2x_0x_1 + 2x_3x_2 \\ 0 & -2x_0x_2 + 2x_3x_1 & 2x_3x_2 + 2x_0x_1 & x_0^2 + x_3^2 - x_2^2 - x_1^2 \end{bmatrix}. \tag{8}$$

It should be noted, that spherical displacements generate a linear three-space on S_6^2. Because we have ∞^3 points in three space, which can serve as centers for spherical displacements, there are ∞^3 three spaces of this type on the Study quadric. The kinematic image of planar displacements could be obtained by setting $y_0 = y_1 = x_2 = x_3 = 0$. The kinematic images of planar displacements also generate three spaces on S_6^2. Because there are ∞^3 planes in three space we have ∞^3 three spaces on of this type on S_6^2.

1.2 Constraint Varieties for Mechanism Analysis and Synthesis

The basic idea to analyze mechanisms with kinematic mapping is the following: every mechanism motion generates a certain set of points, curves, surfaces or higher dimensional algebraic varieties of up to five dimensions in the image space. Generally the dimension of the corresponding variety corresponds to the degree of freedom of the kinematic chain. If for example one point of the moving system of a spatial mechanical device is bound to move on a surface, the system still has five degrees of freedom. Therefore the mechanical constraint is mapped to a hyper-surface in kinematic image space. From this statement we can conclude that every mechanical system in general can be described by a system of algebraic (polynomial) equations.

From algebraic point of view we have a system of polynomial equations $I = (g_1, \ldots, g_n)$, which corresponds to an algebraic variety $V = V(g_1, \ldots, g_n)$. The algebraic varieties are the constraint surfaces. With this interpretation it is possible to use all the progress which was made in recent years in solving systems of polynomial equations (see [8]).

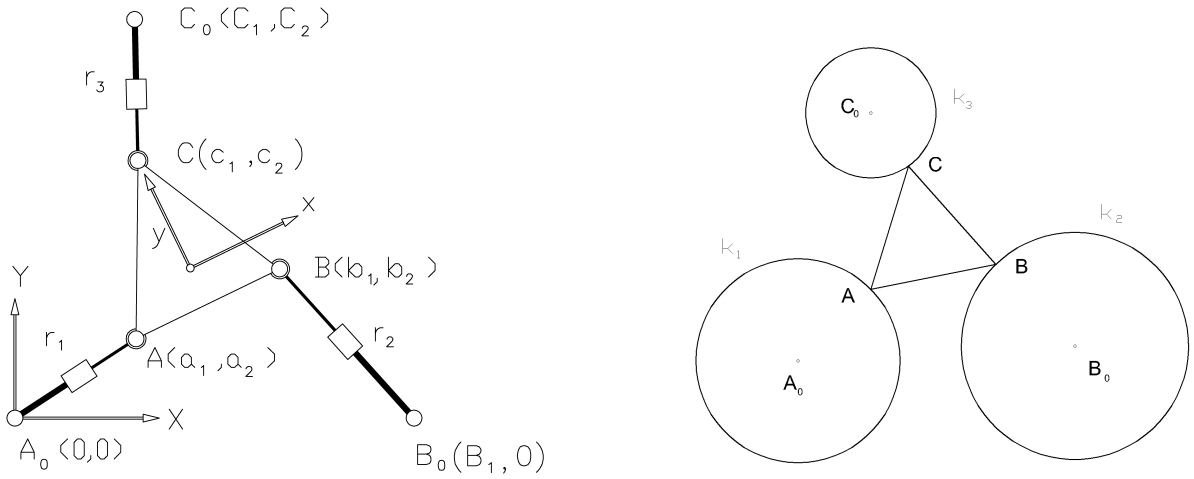

Figure 1: $3RPR$-platform and geometric equivalent

We show this idea with a simple example: consider a planar parallel manipulator consisting of a base and a platform linked by three RPR-legs (Fig.1,left). In the so called direct kinematic we are given the design of the manipulator, i.e. the design of base and platform

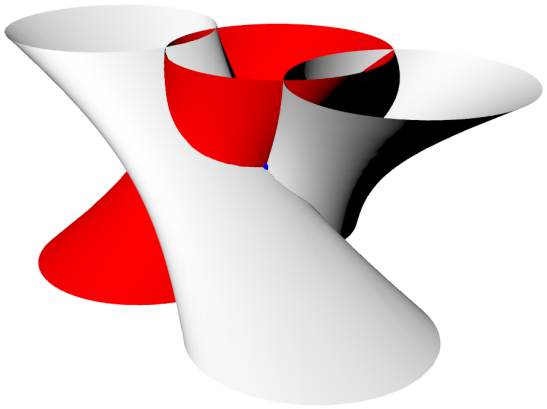

Figure 2: Constraint surfaces in kinematic image space

(the coordinates $(B_1, C_1, C_2, a_1, a_2, b_1, b_2, c_1, c_2)$ and the lengths of the legs r_1, r_2, r_3). The task is to find all assembly modes.

Geometric preprocessing transforms the direct kinematic problem now into the following task: given a triangle and three circles; place the triangle such that its three vertices are on the circles (vertex A on circle k_1 etc., Fig.1,right). The circles also constitute the mechanical constraints. If for a moment we just consider one circle, then we can say for example that mechanically point A is constrained to move on circle k_1. Using planar kinematic mapping this constraint is mapped to a hyper-surface in the three dimensional kinematic image space. It turns out that the constraint surface is a special hyperboloid in this space (Fig.2), Bottema-Roth [6]. Algebraically this hyper-surface is (for the point C):

$$\begin{aligned} h_1: \quad & 4\,{x_2}^2 + 4\,C_2\,x_0\,x_2 + R_3 - 4\,C_1\,x_3\,x_0 - 4\,x_2\,x_0\,c_2 + 4\,x_3\,x_0\,c_1 + 4\,{x_3}^2 - 4\,x_1\,C_2\,x_0\,c_1 + \\ & 4\,x_1\,C_1\,x_0\,c_2 - 4\,x_1\,x_2\,c_1 - 4\,x_1\,C_2\,x_3 - 4\,x_1\,C_1\,x_2 - 4\,x_1\,x_3\,c_2 + 4\,{x_1}^2 C_1\,c_1 + \\ & 4\,{x_1}^2 C_2\,c_2 - 2\,C_2\,c_2 - 2\,C_1\,c_1 = 0 \end{aligned} \tag{9}$$

From algebraic point of view we have three quadratic polynomials h_1, h_2, h_3 which determine the algebraic variety $V = V(h_1, h_2, h_3)$. The dimension of this variety is zero, it consists of 8 points. Six of these points are solution to the direct kinematics problem, two of the points are always complex and do not solve the task.

2 Application to Mechanism Analysis

In this section we show how the above developed theory was applied to mechanism analysis. In a first subsection the direct kinematics of the famous Stewart-Gough platform is solved. In the second subsection we show how the jump of dimension of the solution ideal is related to a jump of the degree of freedom of mechanisms. In the third subsection we apply algebraic geometry, geometric preprocessing and multidimensional geometry to devise a completely

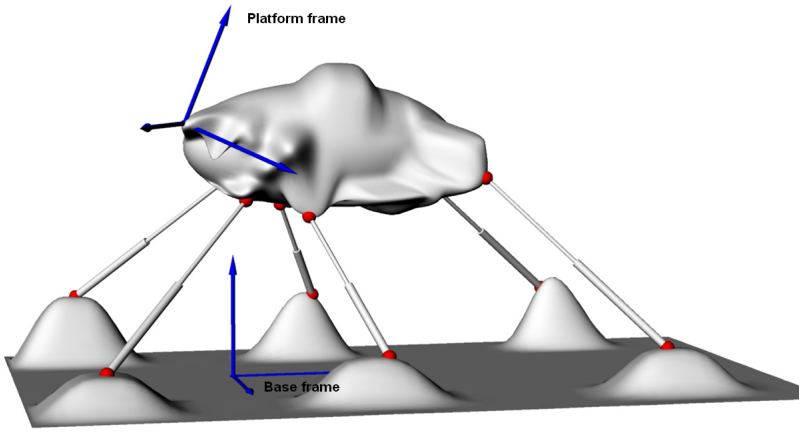

Figure 3: Sketch of a Stewart-Gough Platform

new algorithm for the inverse kinematics of all serial 6R chains (including the most general ones).

2.1 Direct Kinematics of Stewart-Gough Platforms

In this subsection we show how the above mentioned theory is applied to the direct kinematics of Stewart-Gough platforms (SGP) (see Merlet [20], Fig. 3). Similar to the case of planar $3RPR$-platforms it was shown in Husty [12] that the direct kinematics of all SGPs ($6SPS$-platforms, S is a spherical joint, P is a prismatic joint; the prismatic joint is actuated) is governed by a set of seven quadratic equations, one of them being Eq. 4 and the other six having the general form

$$\begin{aligned} h =& R(x_0^2+x_1^2+x_2^2+x_3^2)+4(y_0^2+y_1^2+y_2^2+y_3^2)-2x_0^2(Aa+Bb+Cc)+2x_1^2(-Aa+Bb+Cc)+\\ & 2x_2^2(Aa-Bb-Cc)+2x_3^2(Aa+Bb+Cc)+2x_3^2(Aa+Bb-Cc)+4[x_0x_1(Bc-Cb)+\\ & x_0x_2(Ca-Ac)+x_0x_3(Ab-Ba)-x_1x_2(Ab+Ba)-x_1x_3(Ac+Ca)-\\ & x_2x_3(Bc+Cb)+(x_0y_1-y_0x_1)(A-a)+(x_0y_2-y_0x_2)(B-b)+(x_0y_3-y_0x_3)(C-c)+\\ & (x_1y_2-y_1x_2)(C+c)-(x_1y_3-y_1x_3)(B+b)+(x_2y_3-y_2x_3)(A+a)]=0, \end{aligned} \tag{10}$$

where (a,b,c) are the coordinates of a point in the platform frame, (A,B,C) are coordinates of a point in the base frame, r is the joint parameter (leg length). Furthermore it was set

$$R := A^2+B^2+C^2+a^2+b^2+c^2-r^2.$$

The solutions of the seven quadratic equations constitute an affine variety $V(h_i, S_6^2)$. This variety V represents the solutions of the direct kinematics in the kinematic image space. The polynomials determining V generate an ideal, whose elements are obtained by linear

combination and multiplication of the seven polynomials with coefficients from $\mathbb{R}$. In the general situation the variety V will be zero dimensional, because we have seven equations and seven unknowns. It is well known, that this system has maximal 40 real solutions ([26], [22]). An algorithm to solve the system was presented in [12]. Quite recently it was shown, that within the ideal one can generate additional polynomials which represent additional constraints between the rigid bodies. The zeros of these additional polynomials determine quadrics which pass through all forty solutions. From this follows that one can construct redundant SGP (more than six legs; for anchor points in two different planes (SGPP) even infinitely many) having all solutions of the direct kinematics in common. This has also the consequence that adding leg would not change the singularities of such a SGP. It shows that one has to be careful in adding legs to avoid singularities (see [19]).

2.2 Architecture Singularity and Self Motions of Platform Manipulators (Griffis-Duffy Platforms)

It is not surprising that for special platform and base geometries it can happen that the solution variety V is not zero dimensional. Then $V(h_i, S_6^2)$ no longer consists of discrete points, but of a curve, or even of a surface on S_6^2. Platform manipulators having this property can perform a self motion without actuating the prismatic joints [1]. In the following we discuss such an example. In [10] and [9] two types of mechanisms are proposed which will be called Griffis-Duffy Platforms (GDP). Both are special types of SGP. One of them is called "midline to apex" embodiment and the other "apex to apex" embodiment. The anchor points of the spherical joints on platform and base are arranged on the vertices of a triangle and the remaining three each on the edges of the triangle. Here we will summarize briefly the results of [14] on the "midline to apex" embodiment (Fig. 4). Base and platform consist of an equilateral triangle and the remaining anchor points are the mid points of the three edges. This special case of GDP will be called a "Special Griffis-Duffy-Platform" (SGDP). Using the coordinate systems shown in Fig. 4 coordinates of both anchor points in base and platform are listed in the table of Fig. 5.

2.2.1 Architecture Singularity

For an arbitrary SGP the transformation of the joint velocities into the infinitesimal twist of the produced motion is written as

$$\mathbf{Jq} = \mathbf{t}, \tag{11}$$

where $\mathbf{q}$ is the vector of joint velocities and $\mathbf{t}$ is the twist of the platform. $\mathbf{J}$ is a 6×6-matrix and it is well known that its rows consist of the axis coordinates of the linear actuator axes $\overline{P_i p_i}$. $\mathbf{p_i}^0$ denotes the position of a joint center of the platform measured in the base

[1] Examples of 2-DOF self motions are also known. If non-trivial 3-DOF self motions are possible is not known. They would correspond to solids on S_6^2.

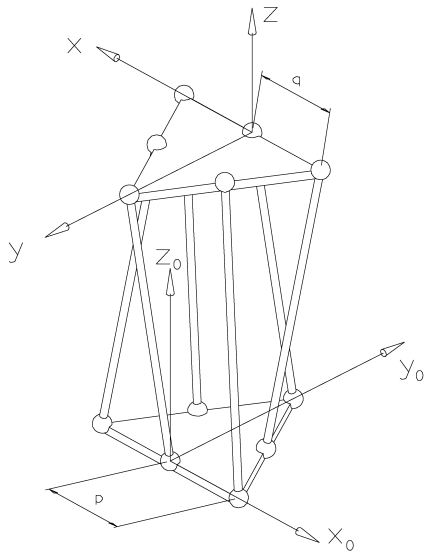

Figure 4: Griffis-Duffy platform

	A	B	C		a	b	c
P_1	-p	0	0	p_1	$\frac{q}{2}$	$\frac{q\sqrt{3}}{2}$	0
P_2	0	0	0	p_2	0	$q\sqrt{3}$	0
P_3	p	0	0	p_3	$-\frac{q}{2}$	$\frac{q\sqrt{3}}{2}$	0
P_4	$\frac{p}{2}$	$\frac{p\sqrt{3}}{2}$	0	p_4	$-q$	0	0
P_5	0	$p\sqrt{3}$	0	p_5	0	0	0
P_6	$-\frac{p}{2}$	$\frac{p\sqrt{3}}{2}$	0	p_4	q	0	0

Figure 5: Coordinates of anchor points

coordinate system and $\mathbf{Q}$ is the transformation matrix from platform to base.

$$\mathbf{p_i^0} = \mathbf{Q}\mathbf{p_i}. \tag{12}$$

To compute the Jacobian matrix $\mathbf{J}$ for the SGDP we substitute the coordinates of the table in Figure 5 into Eq. 12, compute $\mathbf{p_i}^\mathbf{0}$ and the axis coordinates of the legs. For the first leg we get

$$\begin{aligned}
&\Big(0 : p\,(2y_0x_3 - 2y_3x_0 + 2y_2x_1 - 2y_1x_2 + qx_1x_3 + qx_0x_2 - q\sqrt{3}x_2x_3 q\sqrt{3}x_0x_1) : \\
&- p\,(2y_0x_2 - 2y_2x_0 + 2y_1x_3 - 2y_3x_1 + (x_1x_2 - x_0x_3)q + \frac{1}{2}(x_0^2 - x_1^2 + x_2^2 - x_3^2)q\sqrt{3}) : \\
&2y_0x_1 - 2y_1x_0 + 2y_3x_2 - 2y_2x_3 + \frac{1}{2}(x_0^2 + x_1^2 - x_2^2 - x_3^2)q + (x_1x_2 + x_0x_3)q\sqrt{3} + p : \\
&2y_0x2 - 2y_2x_0 + 2y_1x_3 - 2y_3x_1 + (x_1x_2 - x_0x_3)q + \frac{1}{2}(x_0^2 - x_1^2 + x_2^2 - x_3^2)q\sqrt{3} : \\
&2y_0x_3 - 2y_3x_0 + 2y_2x_1 - 2y_1x_2 + qx_1x_3 + qx_0x_2 + q\sqrt{3}x_2x_3 - q\sqrt{3}x_0x_1\Big).
\end{aligned} \tag{13}$$

Similar expressions build up the whole matrix $\mathbf{J}$. Using an algebraic manipulation system to compute the determinant of $\mathbf{J}$ we get $\det \mathbf{J} = 0$. This tells that $\mathbf{J}$ is singular independently of the joint parameters and therefore of the pose of the platform. The SGDP is architecture singular, that means it is singular in every pose of its workspace!

2.2.2 Self Motions of SGDP

In this section we will show that the SGDP platform is not only architecture singular but also movable from every point of its workspace without actuating the joints. To show this

we will go back to the constraint equation Eq. 10 and the equation for S_6^2 (Eq.4). Because of the six legs there are six constraint equations $h_j, j = 1, \ldots, 6$ and S_6^2. They make a system $\mathcal{A}$ of seven quadratic equations that has to be solved for the eight homogeneous unknowns $x_i, y_i,\ (i = 0, \ldots, 3)$. To admit a self-motion the affine variety $V(h_j, S_6^2)$ consisting of the zeros of the polynomial equations $h_j = 0, x_0y_0 + x_1y_1 + x_2y_2 + x_3y_3 = 0$ has to be at least one dimensional. We will show that V is a curve. This curve represents in the kinematic image space the one parameter motion which the platform can perform without changing leg lengths. Substituting the coordinates of the table in Figure 5 into Eq. 10 we get six constraint equations $h_j,\ (j = 1, \ldots, 6)$ one of them, h_1, is displayed below, all the other five have a similar structure.

$$\begin{aligned} h_1 : {} & qx_0^2p + 4y_0x_1p - 4y_1x_0p - 4y_3x_2p + 4y_2x_3p - qx_3^2p - 2q\sqrt{3}x_0x_3p + qx_1^2p - qx_2^2p + \\ & 2q\sqrt{3}x_1x_2p + (x_3^2 + x_1^2 + x_0^2 + x_2^2)R_1 + 2x_2y_3q - 2y_2x_3q + 2y_0x_1q - 2y_1x_0q + \\ & 2y_1x_3q\sqrt{3} + 2x_2y_0q\sqrt{3} - 2y_2x_0q\sqrt{3} - 2y_3q\sqrt{3}x_1 + 4(y_3^2 + y_2^2 + y_0^2 + y_1^2) = 0. \end{aligned} \tag{14}$$

From the six constraint equations five difference equations are produced: $U_1 = h_1 - h_3, U_2 = h_2 - h_5, U_3 = h_4 - h_6, U_4 = h_1 - h_2, U_5 = h_1 - h_4$. The equations U_i have the characteristic property that they are all linear in y_i. We take three of the difference equations U_1, U_2, U_3 and Eq. 4 and solve this linear system $\mathcal{LS}$ for y_i. Substitution of the solutions of $\mathcal{LS}$ into U_4, U_5 and h_1 yields a system $\mathcal{S}$ of three nonlinear equations for the four remaining homogeneous unknowns x_i. It is easy to show that no more independent equations can be generated from the original system $\mathcal{A}$. A close inspection of the new system $\mathcal{S}$ shows that U_4 is of degree four, h_1 is of degree eight and U_5 takes the form

$$U_5 : \quad (x_0^2 + x_1^2 + x_2^2 + x_3^2)(3q^2 - 3p^2 - R_4 - R_2 - R_6 + R_3 + R_1 + R_5) = 0. \tag{15}$$

The first factor in U_5 cannot be zero because the x_i are the Euler parameters of a Euclidean displacement and the second factor depends only on the design of the manipulator and the leg lengths. We will call the second factor an *assembly condition*, because U_5 allows only one interpretation: Either U_5 is fulfilled, which means one linear condition on the legs is fulfilled, or this condition is not fulfilled, but then the manipulator cannot be assembled with the six given legs. Let us assume that U_5 is fulfilled. Then only two equations remain in $\mathcal{S}$ for four homogeneous unknowns. One of the unknowns e.g. x_1 can be eliminated and the remaining equation $L(x_0, x_2, x_3, R_2, R_3, R_4, R_5, R_6) = 0$ represents the affine solution variety V of the original set of seven nonlinear equations. After specifying a set of joint parameters $(R_2, R_3, R_4, R_5, R_6)$ the equation $L(x_0, x_2, x_3) = 0$ represents a curve in the Study parameter space which corresponds to a one parameter motion which the platform will perform without changing the joint inputs. Inspection of L reveals that it has special algebraic (and geometric) properties because it can be factored into

$$L : \quad p^{20}(x_0, x_2, x_3)(q^6(x_0, x_2, x_3))^2 = 0. \tag{16}$$

q^6 is a sixth degree polynomial (which is squared) and it corresponds to the determinant D of coefficients of the linear system $\mathcal{LS}$ which has been used to solve for y_i. This polynomial

cannot vanish in the case in discussion, so the motion is represented by the polynomial of degree 20. Different subcases can occur for different values of leg lengths because then D could vanish and the elimination process has to be modified. A detailed discussion can be found in [14]. Note that the polynomial of degree 20 in Eq. 16 does not necessarily show the order of the overall motion curve because it represents only a projection of this curve onto the x_2x_3 plane of the Euler parameter space. A detailed discussion on this fact is in [27] where continuation methods are used to find all components of different dimensions of the solution variety V.

2.3 Kinematic Image of a 3R Serial Chain

The most important step in a recently developed algorithm for the inverse kinematics of an open $6R$-chain [15, 16], is the decomposition of the $6R$-chain into two $3R$-chains. Therefore, at first we will study the kinematic image of the $3R$-chain and derive some of its geometric properties.

Given the design (the Denavit-Hartenberg-parameters [DH-parameters]) of an arbitrary $3R$-chain we can compute the relative position of the end-effector frame Σ with respect to a base frame Σ_0 in dependence of three rotation angles u_1, u_2, u_3. Therefore, the constraint manifold of a $3R$-chain, representing all poses the frame Σ can attain is a 3-manifold in the kinematic image space.

It is known (see [23]) that the constraint manifold representing a $2R$-chain in the kinematic image space is the intersection of a 3-space T with the Study quadric S_6^2. This fact has been used in [7] to derive a new method for the synthesis of Bennett mechanisms. The intersection of S_6^2 and T is again a quadric surface.

If we fix one of the three revolute joints of the $3R$-chain by fixing one parameter, say u_3, we get a $2R$-chain. Its kinematic image lies in a 3-space T. Hence, the constraint manifold of the $3R$-chain is the intersection of the Study-quadric S_6^2 with a one parameter set of 3-spaces $T(u_3)$.

If we fix two of the three revolute joints of the $3R$-chain by fixing the parameters u_1 and u_2, we get a pure rotation about the third revolute axis. This rotation maps to a line l on the Study quadric. The line l itself depends on the two parameters u_1 and u_2; therefore we write $l = l(u_1, u_2)$. The points on l are parameterized by u_3. We have a closer look at this parametrization:

The parametric representation of the constraint manifold of the $3R$-chain in kinematic image space, as computed via (6) and (7), reads $\mathbf{p}(u_1, u_2, u_3)$. We apply the half-tangent substitution $v_i = \tan(u_i/2)$, thus obtaining a rational parametric representation $\mathbf{p}(v_1, v_2, v_3)$ of degree four. Fixing v_1 and v_2 yields a rational parametrization $\mathbf{p}(v_3)$ of the straight line $l(v_1, v_2)$.

Lemma 1 *For any v_1, v_2, the parametric representation $\mathbf{p}(v_3)$ of $l(v_1, v_2)$ is linear in v_3.*

A proof of this lemma can be found in [16].

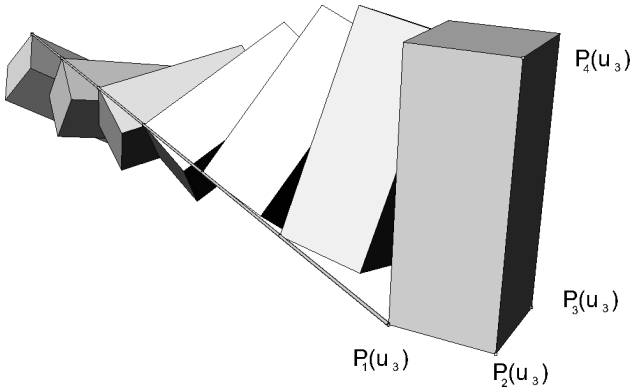

Figure 6: Symbolic figure of SM_3

The 3-spaces $T(v_3)$ can be generated in the following way: We choose four fixed straight lines $l(v_{1,i}, v_{2,i})$, parameterized by $\mathbf{p_i}(v_3)$ $(i = 1, \ldots, 4)$. Every 3-space $T(v_3)$ is spanned by $\mathbf{p_1}(v_3), \ldots, \mathbf{p_4}(v_3)$. On the other hand, a straight line $l(v_1, v_2)$ is the span of two points $\mathbf{p_j}(v_1, v_2) \in T(v_{3,j})$. The relation between the points $\mathbf{p_j}(v_1, v_2)$ can be extended to a unique projective transformation $\pi\colon T(v_{3,1}) \to T(v_{3,2})$ such that $\pi(\mathbf{p_1}(v_1, v_2)) = \mathbf{p_2}(v_1, v_2)$ for all v_1, v_2. Any straight line spanned by corresponding points $\mathbf{x} \in T(v_{3,1})$ and $\pi(\mathbf{x}) \in T(v_{3,2})$ intersects all 3-spaces $T(v_3)$ and any four of these lines can be used to generate the 3-spaces $T(v_3)$.

The one parameter set of 3-spaces $T(v_3)$ generated as above is known in geometry as a *Segre manifold*. A Segre manifold is also defined as topological product of two linear spaces, i.e., the manifold of all ordered pairs of points of both spaces (see [21, p. 569]).

So far, we always fixed the rotation angle $v_3 = \tan(u_3/2)$ of the third revolute joint, thus obtaining a Segre manifold that will be denoted by SM_3. Of course we can also fix v_1 or v_2. This yields two different one parameter sets of 3-spaces and two different Segre manifolds SM_3', SM_3''. We summarize the above considerations in

Theorem 1 *The constraint manifold of a $3R$-chain is the intersection of the Study quadric with a Segre manifold* SM_3 (SM_3', SM_3'')*, generated by two projectively coupled 3-spaces T_1, $T_2 \subset P^7$. The intersection of T_i with the Study quadric S_6^2 is the kinematic image of a $2R$-chain obtained by fixing the rotation angles u_3 (u_1, u_2) of the $3R$-chain.*

A symbolic sketch of SM_3 is depicted in Fig. 6.

2.3.1 Intersection of hyper-planes

A 3-space in the seven dimensional projective kinematic image space is geometrically determined by intersecting four hyper-planes $H_1, \ldots, H_4$. Algebraically this means it is given by four linear equations. We will describe every 3-space $T(v_3)$ in this way. The Segre manifold is then the intersection of four hyper-planes, each depending on the parameter v_3. This

representation will be used in the proposed algorithm for the inverse kinematics of an open $6R$-chain in Section 2.3.2.

For each of the four hyper-planes $H_j(v_3)$ four points $\mathbf{p_i}(v_3)$ are given; but they do not determine $H_j(v_3)$. Because seven points span a hyper-plane in P^7 we need three more points $\mathbf{a_{j,1}}$, $\mathbf{a_{j,2}}$, $\mathbf{a_{j,3}} \in H_j(v_3)$ to compute a linear equation of $H_j(v_3)$. In principle, the points $\mathbf{a_{j,k}}$ can be taken anywhere in P^7 but it makes sense to choose them such that the resulting hyper-plane equations become as simple as possible. Without loss of generality we take the three points such that $\mathbf{a_{j,k}} \in \mathrm{SM}_3 \cap S_6^2$. We choose the points $\mathbf{a_{j,k}}$ independent of v_3; there exist fixed parameter values v_3^{jk} such that $\mathbf{a_{j,k}} \in T(v_3^{jk})$.

The points $\mathbf{p_i}(v_3)$ and $\mathbf{a_{j,k}}$ have coordinate vectors

$$\mathbf{p_i}(v_3) = [p_{i0}, \ldots, p_{i7}]^T, \quad \mathbf{a_{j,k}} = \left[a_0^{jk}, \ldots, a_7^{jk}\right]^T.$$

Note that the coordinates of $\mathbf{p_i}$ depend linearly on v_3, although this does not reflect in our notation. The equation of a hyper-plane $H_j(v_3)$ is given by the Grassmannian determinant

$$H_j(v_3)\colon \quad \det \begin{bmatrix} x_0 & x_1 & x_2 & x_3 & y_0 & y_1 & y_2 & y_3 \\ p_{10} & p_{11} & p_{12} & p_{13} & p_{14} & p_{15} & p_{16} & p_{17} \\ \vdots & & & & & & & \vdots \\ p_{40} & p_{41} & p_{42} & p_{43} & p_{44} & p_{45} & p_{46} & p_{47} \\ a_0^{j1} & a_1^{j1} & a_2^{j1} & a_3^{j1} & a_4^{j1} & a_5^{j1} & a_6^{j1} & a_7^{j1} \\ a_0^{j2} & a_1^{j2} & a_2^{j2} & a_3^{j2} & a_4^{j2} & a_5^{j2} & a_6^{j2} & a_7^{j2} \\ a_0^{j3} & a_1^{j3} & a_2^{j3} & a_3^{j3} & a_4^{j3} & a_5^{j3} & a_6^{j3} & a_7^{j3} \end{bmatrix} = 0. \tag{17}$$

We denote the coefficients of the hyperplane equations (17) by c_{jl}, i.e.,

$$H_j(v_3)\colon c_{j0}x_0 + c_{j1}x_1 + c_{j2}x_2 + c_{j3}x_3 + c_{j4}y_0 + c_{j5}y_1 + c_{j6}y_2 + c_{j7}y_3 = 0. \tag{18}$$

The coefficients c_{jl} are polynomials of degree four in v_3 and can be interpreted as homogeneous coordinates for the hyperplane H_j. Because of the special choice of the points $\mathbf{a_{j,k}}$, the polynomials c_{jl} have the common divisor

$$g = (v_3 - v_3^{j1})(v_3 - v_3^{j2})(v_3 - v_3^{j3}). \tag{19}$$

Dividing the polynomials c_{jl} by g yields hyperplane coordinates for $H_j(v_3)$ that depend linearly on v_3. We state this as

Theorem 2 *The Segre manifold* SM_3 *is the intersection of four one parameter pencils of hyperplanes* $H_j(v_3)$. *The hyperplane coordinates of* $H_j(v_3)$ *depend linearly on* v_3.

Remark 2 *It is even possible to compute symbolically the hyperplane coordinates of* $H_j(v_3)$ *without specifying the DH-parameters of the* $3R$*-robot. Computed once the equations can be taken for every possible design.*

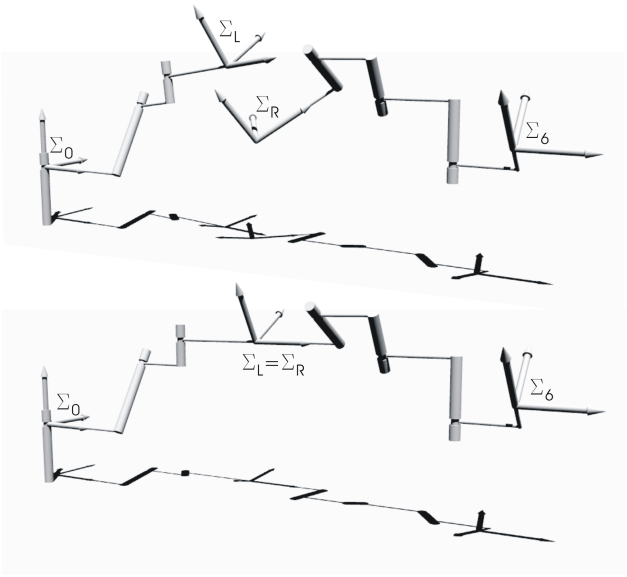

Figure 7: Cutting of the $6R$ into two $3R$ serial chains

2.3.2 Discussion of the Inverse Kinematics of General 6R-Manipulators

In this subsection we show how the constraint manifolds of $3R$-chains can be used to solve the inverse kinematics of a general open $6R$ manipulator. Recall that in the inverse kinematic problem of a serial chain the design and a pose of the end-effector of the manipulator is known. The rotation angles u_i of the revolute joints have to be computed. To apply the theory developed in the last section we break up the link between the third and the fourth revolute joint of the $6R$ and attach two copies of a coordinate frame $\Sigma_L = \Sigma_R$ (the "left" and the "right" frame) in the middle of the common normal of these two joints such, that the twist angle between the z-axes of Σ_3 and $\Sigma_L = \Sigma_R$ is $\frac{\alpha_3}{2}$ (Fig. 7). Then we compute the direct kinematics for the first half of the $6R$ manipulator, which is now a $3R$-chain, with the end-effector frame Σ_L.

When the end-effector of the $6R$ manipulator is fixed we can do the same with the second part of the $6R$ but in the opposite direction. This means that for this $3R$ manipulator Σ_6 is the base and Σ_R is the end-effector frame.

$\mathrm{SM}_{3,L}$ is a Segre manifold in P^7. We saw that $\mathrm{SM}_{3,L}$ is the intersection of four one-parameter sets of hyperplanes. The same is true for $\mathrm{SM}_{3,R}$. Hence, we have to intersect eight one parameter sets of hyper-planes with S_6^2. We summarize these results in

Theorem 3 *Geometrically the inverse kinematics of a general $6R$-serial chain is equivalent to the intersection of eight one parameter sets of hyper-planes with S_6^2.*

An investigation of the algebraic structure of the nine equations reveals the non linearity of the problem. We have eight hyper-plane equations $H_i(v_3) = 0$, $H_{i+4}(v_6) = 0$, $i = 1, \ldots, 4$ and Equation (4) of S_6^2. The equations H_i are linear in x_i, y_i and bilinear in $x_i v_3$ and $y_i v_3$

resp. $x_i v_6$ and $y_i v_6$. The solution algorithm of this system is straight forward. The complete solution can be found in [16].

3 Synthesis of Mechanism

Kinematic mapping can also be used in the synthesis of mechanisms. A detailed introduction into this interesting topic can be found in [18]. The mathematical tools used there are closely related to the presented methods within this paper. But there is a difference in the geometric interpretation of the devised equations. We show the application of our methods in the synthesis of a Bennett mechanism.

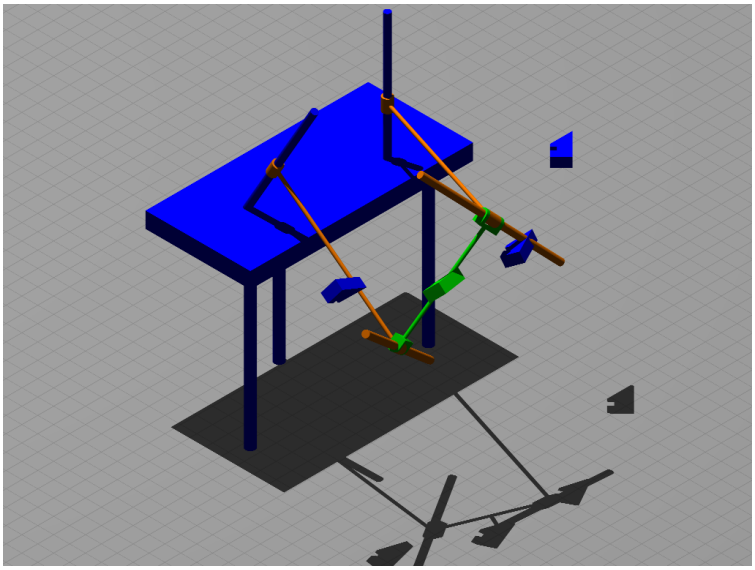

Figure 8: Bennett mechanism

The Bennett mechanism is a closed $4R$-chain. It is well known that a Bennett mechanism can be synthesized exactly when three poses of the end effector system are given (Fig.8). Synthesis means that we have to find the design parameters of the mechanism and the location of the axes in the fixed system and the location of the moving body in the moving system. For the synthesis of such a mechanism we attach two of the revolute axes to the fixed system and two axes to the moving (coupler) system. Now we prize open the coupler link and obtain two open RR-chains. The basic idea of the synthesis is now: We map the possible displacements of the first RR-chain onto S_6^2. This yields the constraint manifold $\mathcal{M}_1$ of the RR-chain in the kinematic image space. The same procedure we perform with the other RR-chain and obtain a second constraint manifold $\mathcal{M}_2$. Possible assembly modes of the two RR-chains correspond to intersection points of $\mathcal{M}_1$ and $\mathcal{M}_2$.

3.1 Constraint Manifold of RR-Chains

Using the Denavit-Hartenberg notation we compute the forward kinematics of the RR-chain. This yields a coordinate transformation of the type

$$\mathbf{x}'(u_1, u_2) = \mathbf{A}(u_1, u_2)\mathbf{x} + \mathbf{t}(u_1, u_2). \tag{20}$$

u_1 and u_2 are the rotation parameters of the two rotations about the axes of the RR-chain. We apply the procedure explained in Section 1.1 to obtain the Study-parameters which are in this case functions of two parameters u_1, u_2:

$$x_i = f_i(u_1, u_2), \qquad y_i = g_i(u_1, u_2), \qquad i = 0, \ldots 3. \tag{21}$$

Elimination of the two parameters yields five equations in the unknowns x_i, y_i, $i = 0, \ldots, 3$. It turns out that four equations are linear and one equation is the equation of the Study-quadric S_6^2. This result agrees with Selig [23], who derived a normal form of the equations using dual quaternions and exponential mapping. The multidimensional interpretation of the five equations is as follows: each linear equation describes a (six dimensional) hyperplane L^6 of P^7. The intersection of these hyper-planes is a linear three-plane L^3. This means that all possible poses of the end-effector of the RR-chain are in L^3. Note that not all $L^3 \subset P^7$ correspond to RR-chains. The constraint manifold $\mathcal{M}$ of an RR-chain is therefore the intersection of L^3 and S_6^2.

With this knowledge we have a much simpler algorithm to derive the five linear equations describing $\mathcal{M}$: Each three-plane (i.e. a three dimensional space) is determined by four points. To find the four linear equations we choose four discrete sets of rotation angles $u_1^i, u_2^i, i = 1, \ldots, 4$. These four sets correspond to four points P_i on the Study-quadric. Now we construct four arbitrary hyper-planes L^6 containing the four points P_i. This is done by adding three arbitrary points $Q_j^k, j = 1, \ldots, 3$, $k = 1, \ldots, 4$ of P^7 different for each hyperplane and computing the Grassmann determinant:

$$E_i = \begin{vmatrix} x_0 & x_1 & x_2 & x_3 & y_0 & y_1 & y_2 & y_3 \\ p_{i0} & p_{i1} & p_{i2} & p_{i3} & p_{i4} & p_{i5} & p_{i6} & p_{i7} \\ q_{j0}^k & q_{j1}^k & q_{j2}^k & q_{j3}^k & q_{j4}^k & q_{j5}^k & q_{j6}^k & q_{j7}^k \end{vmatrix} = 0, \quad i = 1, \ldots, 4,\ j = 1, \ldots 3,\ k = 1, \ldots, 4. \tag{22}$$

Due to the fact that a Bennett mechanism consists of two RR-chains, one has to intersect two three-planes L_1^3, L_2^3 in P^7. According to the well known dimension formula

$$\dim(U \cap V) = \dim(U) + \dim(V) - \dim(U + V) \tag{23}$$

where U, V denote sub-spaces of an n-dimensional space P^n, the intersection of two three-planes L_1^3, L_2^3 in a seven dimensional space P^7 can be:

- $\dim(L_1^3 \cap L_2^3) = -1, \Rightarrow$ intersection is empty,
- $\dim(L_1^3 \cap L_2^3) = 0, \Rightarrow$ intersection is one point,

- $\dim(L_1^3 \cap L_2^3) = 1, \Rightarrow$ intersection is a line,
- $\dim(L_1^3 \cap L_2^3) = 2, \Rightarrow$ intersection is a two-plane
- $\dim(L_1^3 \cap L_2^3) = 3 \Rightarrow L_1^3$ and L_2^3 coincide.

The first case is the general case. The mechanical interpretation is that two general RR-chains never can be assembled to form a closed $4R$-mechanism. There have to be conditions to make this happen. When the constraint manifolds are chosen such that they come from a $4R$-chain, then they have exactly one point in common, which is on S_6^2 (forward kinematics of a serial $4R$-chain). This fact is also a simple proof that the inverse kinematics of a general $4R$ serial chain has one solution. The case of the line intersection is only possible for special $4R$-chains for which the inverse kinematics then has two solutions, which correspond to the two intersections of the line with S_6^2. As we know, the Bennett motion is a one-parameter-motion, represented by a curve in the kinematic image space. Therefore only the cases of a line, which lies completely on S_6^2 or a two-plane are of interest. The case that the line is contained in S_6^2 is not possible. Following Baker[2], who argued via screws, the relative motion between opposite links of a proper Bennett loop can be neither purely rotational nor purely translational at any time. Since straight lines on S_6^2 correspond to rotations or translations we can restrict ourselves to the case of $\dim(L_1^3 \cap L_2^3) = 2$. The kinematic image of the Bennett motion is therefore the intersection of a two-plane with the Study-quadric S_6^2. This yields another confirmation of the fact that the synthesis of a Bennett needs three precision points. Three precision points correspond to three points on the Study-quadric and span the two-plane. This agrees with [25]. Summarizing we have:

Theorem 4 *Bennett motions are represented by planar sections of the Study-quadric and vice versa.*

The intersection of the two-plane and S_6^2 is a quadratic curve. In this sense Bennett motions can be regarded as the simplest non-trivial one parameter space motions. A direct consequence of the above considerations is the following

Corollary 1 *Bennett linkages are the only movable $4R$-chains.*

It should be noted that to the authors' best knowledge up to now there exist only complicated algebraic proofs of this result (see for example [17]). A complete discussion of the synthesis algorithm including an example can be found in [7].

4 Conclusion

In this overview we have discussed the application of kinematic mapping and the resulting geometric-algebraic approach to solve problems in mechanism analysis and synthesis. It was shown that geometric preprocessing in a multidimensional setting allowed to simplify and subsequently solve the sets of polynomial equations linked to the mechanical problems.

5 Acknowledgements

The author is grateful to his colleagues H.-P. Schöcker, K. Brunnthaler and M. Pfurner for giving the consent to use their results in this overview.

References

[1] Angeles, J., Fundamentals of Robotic Mechanical Systems. Theory, Methods and Algorithms, Springer, New York, 1997.

[2] Baker, J. E. 1998. On the motion geometry of the Bennett linkage. Proceedings of the 8th International Conference on Engineering Computer Graphics and Descriptive Geometry. Austin. Texas. USA. pp. 433–437.

[3] Bennett, G. T. 1903. A new mechanism. Engineering. Vol. 76. pp. 777–778.

[4] Bennett, G. T. 1913–1914. The scew isogram-mechanism. Proceedings of the London Mathematical Society. Vol. 13. pp. 151–173.

[5] Blaschke, W. 1960, *Kinematik und Quaternionen*, Wolfenbüttler Verlagsanstalt.

[6] Bottema, O., Roth, B., 1990, *Theoretical Kinematics*, Dover Publishing.

[7] Brunnthaler, K., Schröcker, H.-P., Husty, M. L., A new method for the synthesis of Bennet mechanisms, in: Proceedings of CK 2005, Cassino, Italy, 2005.

[8] Dickenstein, A. Emiris, I.Z., Solving Polynomial Equations, Foundations, Algorithms and Applications, Springer Pub., 2005.

[9] Griffis, M., Crane, C., Duffy, J., 1994, "A smart kinestatic interactive platform", in: Lenarcic, J. and Ravani, B.: *Advances in Robot Kinematics*, Kluwer Acad. Pub., 459 – 464, ISBN 0-7923-2983-X.

[10] Griffis, M., Duffy, J., 1993, "Method and Apparatus for Controlling Geometrically Simple Parallel Mechanisms with Distinctive Connections", US Patent # 5,179, 525, 1993.

[11] Harris, J. , Algebraic Geometry: A First Course, Vol. 133 of Graduate Texts in Mathematics, Springer, 1995.

[12] Husty, M. L., 1996, "An Algorithm for Solving the Direct Kinematic of General Stewart-Gough Platforms",*Mechanism and Machine Theory*, vol. 31, No. 4, pp. 365-380.

[13] Husty, M. L., Karger A., Sachs H., Steinhilper W., Kinematik und Robotik, Springer-Verlag, Berlin, Heidelberg, New York, 1997.

[14] Husty, M.L„ and Karger, A., 2000 "Self-Motions of Griffis-Duffy Type Platforms", *Proceedings of IEEE conference on Robotics and Automation (ICRA 2000)*, San Francisco, 7–12.

[15] Husty, M. L. - Pfurner, M. - Schröcker, H.P., A New and Efficient Algorithm for the Inverse kinematics of a General 6R, Proceedings of IDETEC/CIE 2005, DETEC/MECH-84745, 2005, 8p.

[16] Husty, M. L. - Pfurner, M. - SchrÖCker, H.P., A New and Efficient Algorithm for the Inverse Kinematics of a General 6R, Mech. Mach. Theory, 2006, in print.

[17] Karger, A. 4-parametric robot-manipulators and the Bennett's mechanism. Private communication.

[18] McCarthy J.M., Geometric Design of Linkages, Vol. 320 of Interdisciplinary Applied Mathematics, Springer-Verlag, New York, 2000.

[19] Mielczarek S., Husty M., - Hiller M., Designing a redundant Stewart-Gough platform with a maximal forward kinematics solution set. CD-ROM, Proceedings MUSME, Mexico City, 12 pages, (2002).

[20] Merlet, J.P., 2000, *Parallel Robots*, Kluwer Academic Publishers, Dordrecht, The Netherlands.

[21] Naas J., Schmid H., Mathematisches Wörterbuch, Vol. Band II, Akademie-Verlag Berlin, 1974.

[22] Raghavan, M., 1991, "The Stewart platform of general geometry has 40 configurations", *ASME Design and Automation Conf., Chicago, 1991*, vol. 32-2, 397–402.

[23] Selig,J. M., Geometric Fundamentals of Robotics, Monographs in Computer Science, Springer, New York, 2005.

[24] Study E., Geometrie der Dynamen, B. G. Teubner, Leipzig, 1903.

[25] Suh, C. H., Radcliffe, C. W. 1978. Kinematics and Mechanisms Design. John Wiley and Sons. Canada.

[26] Wampler, C., 1996, "Forward displacement analysis of general six-in-parallel SPS (Stewart) platform manipulators using soma coordinates", *Mech. Mach. theory*, vol.31 (3), 331-337.

[27] Sommese, A, Verschelde, Wampler, Ch., 2002, "Advances in Polynomial Continuation for Solving problems in Kinematics", preprint.